COLD SPRING HARBOR
Molecular Case Studies

RESEARCH REPORT

Expanding the phenotype of *ATP6AP1* deficiency

Subit Barua,[1] Sara Berger,[2] Elaine M. Pereira,[3,4] and Vaidehi Jobanputra[1,4]

[1]Department of Pathology and Cell Biology, Columbia University Irving Medical Center, New York, New York 10032, USA; [2]Division of Clinical Genetics, Department of Pediatrics, Columbia University, Vagelos College of Physicians and Surgeons, New York, New York 10032, USA; [3]Division of Clinical Genetics, Department of Pediatrics, Columbia University Vagelos College of Physicians and Surgeons and NewYork-Presbyterian Morgan Stanley Children's Hospital, New York, New York 10032, USA

Abstract Vacuolar ATPases (V-ATPases) are large multisubunit proton pumps conserved among all eukaryotic cells that are involved in diverse functions including acidification of membrane-bound intracellular compartments. The *ATP6AP1* gene encodes an accessory subunit of the vacuolar (V)-ATPase protein pump. Pathogenic variants in *ATP6AP1* have been described in association with a congenital disorder of glycosylation (CDG), which are highly variable, but often characterized by immunodeficiency, hepatopathy, and neurologic manifestations. Although the most striking and common clinical feature is hepatopathy, the phenotypic and genotypic spectrum of *ATP6AP1-CDG* continues to expand. Here, we report identical twins who presented with acute liver failure and jaundice. Prenatal features included cystic hygroma, atrial septal defect, and ventriculomegaly. Postnatal features included pectus carinatum, connective tissue abnormalities, and hypospadias. Whole-exome sequencing (WES) revealed a novel de novo in-frame deletion in the *ATP6AP1* gene (c.230_232delACT;p.Tyr77del). Although both twins have the commonly reported clinical feature of hepatopathy seen in other individuals with *ATP6AP1-CDG*-related disorder, they do not have neurological sequelae. This report expands the phenotypic spectrum of *ATP6AP1-CDG*-related disorder with both probands exhibiting unique prenatal and postnatal features, including fetal ventriculomegaly, umbilical hernia, pectus carinatum, micropenis, and hypospadias. Furthermore, this case affirms that neurological features described in the initial case series on *ATP6AP1-CDG* do not appear to be central, whereas the prenatal and connective tissue manifestations may be more common than previously thought. This emphasizes the importance of long-term clinical follow-up and variant interpretation using current updated recommendations.

Corresponding author:
vj2004@cumc.columbia.edu

Ontology terms: congenital septal defect; fetal cystic hygroma; jaundice

Published by Cold Spring Harbor Laboratory Press

doi:10.1101/mcs.a006195

INTRODUCTION

Congenital disorders of glycosylation (CDGs) are a rapidly growing group of genetic disorders that affect glycoprotein biogenesis. More than 130 types of CDG have been reported, and more than 140 genes are associated with different types of CDG that include symptoms ranging from mild to severe (Chang et al. 2018; Wilson and Matthijs 2021). A clinical diagnosis of CDG is often challenging because of the highly variable phenotype, broad effect on the function of multiple organs, and overall limited awareness of CDGs (Ng and Freeze 2018).

Vacuolar ATPase (V-ATPase) is a multisubunit rotary nanomotor in the Golgi-endosomal secretory pathway that is ubiquitously expressed (Nishi and Forgac 2002). V-ATPase is

[4]These authors are senior coauthors

essential for luminal acidification of secretory vesicles and to maintain homeostasis in the body (Casey et al. 2010; Pamarthy et al. 2018). Defects in V-ATPase complex and impairment in acidification of Golgi apparatus is predicted to modulate the Golgi-located glycosylation machinery that leads to defects in glycosylation (Guillard et al. 2009). Variants in causative genes (*ATP6V0A2*, *ATP6V1A*, *ATP6V1E1*, and *ATP6AP2*) encoding distinct subunits of V-ATPase are often associated with CGD (Kornak et al. 2008; Rujano et al. 2017; Van Damme et al. 2017; Ondruskova et al. 2020). In addition, a hypomorphic variant in the chaperone protein *VMA21* that is required for V-ATPase assembly was recently reported in association with VMA21-CDG (Cannata Serio et al. 2020). *ATP6AP1* is an accessory subunit of the V-ATPase, and pathogenic variants in *ATP6AP1* have been reported to be associated with X-linked CDG, which was initially characterized by immunodeficiency with hepatopathy and neurological features (Jansen et al. 2016). Additional features that have been reported in case reports published since then include hepatomegaly, splenomegaly, pancreatic insufficiency, hearing loss, aortic dilation, and cutis laxa (Jansen et al. 2016; Dimitrov et al. 2018; Witters et al. 2018; Ondruskova et al. 2020; Song et al. 2020; Tvina et al. 2020). Here, we describe identical twin males with a novel hemizygous variant in the *ATP6AP1* gene, exhibiting overlapping and additional clinical features in both prenatal and postnatal stages. We applied the point-based system for classification of this de novo variant based on current recommendations from The American College of Medical Genetics and Genomics (ACMG)/The Association for Molecular Pathology (AMP) and The Association for Clinical Genomic Science (ACGS) working group (SVI 2018; ACGS 2019).

RESULTS

Clinical Presentation and Family History

The probands are the product of monochorionic-diamniotic twin pregnancy from a father of Guyanese descent and a mother of Italian descent. Consanguinity was denied. There were no similarly affected family members.

First-trimester ultrasounds showed each twin had a cystic hygroma, dilated aorta, and an atrial septum defect. Chorionic villus sampling (CVS) was performed at an outside hospital, and a karyotype, chromosomal microarray, and Noonan syndrome panel were reported to be negative, although copies were not provided for our review. Second-trimester ultrasounds also showed cardiomegaly and borderline ventriculomegaly.

The probands were born at an outside institution at 36 weeks of gestation via cesarean section because of fetal malpositioning. Postnatally, both were noted to have pectus carinatum, umbilical and bilateral inguinal hernias, micropenis, and hypospadias, with twin B's symptoms being more severe. Head ultrasounds and spinal magnetic resonance imagings (MRIs) were normal. Echocardiograms confirmed a septum primum aneurysm and mildly dilated ascending aorta. The twins developed jaundice but did not require phototherapy. After a 5-day neonatal intensive care unit (NICU) stay, they were discharged with close outpatient follow-up.

At 2 months of age they both had noticeable jaundice. Workup showed elevated bilirubin levels and abnormal liver function with ultrasounds concerning for gallstones, left liver lobe prominence, and ascites. Both probands were admitted to our institution for further evaluation. Plasma amino acids were within normal limits, whereas urine organic acids showed elevated levels of 4-hydroxy phenyllactic acid and 4-hydroxy phenylpyruvic acid. Twin B experienced encephalopathy with hyperammonemia. Given the above, a genetic consult was initiated. Because of the dysmorphic features, skin laxity around the epigastric region, flank, and groin (see Fig. 1A–F), and abnormal liver function, whole exome sequencing was initiated.

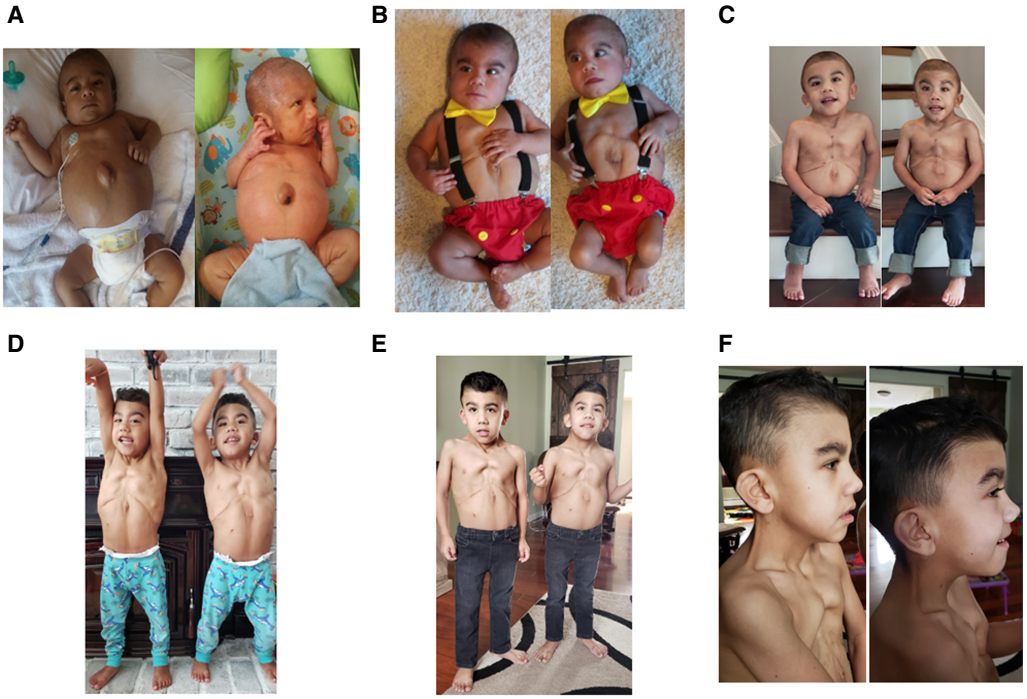

Figure 1. (*Left*) Twin A and (*right*) twin B. (*A*) In infancy both twins exhibit significant abdominal distention and umbilical hernias. In Twin B the skin laxity of the legs is visible bilaterally. (*B*) Pictures of the twins from 1 to 3 years of age. At 1 year, the significant pectus carinatum is noticed in both twins. There is excess skin around the umbilical hernias. Their abdomens remain prominent. (*C*) At 2 years, webbing is noted more so on twin B (*right*). There is significant skin laxity over the abdomen near scarred areas. (*D*) At 3 years, with their arms raised, there is laxity appreciated in the axillary areas. The abdominal scarring is healed but prominent. (*E*) At 4 years, they continue to have coarse facial features, epicanthal folds bilaterally, and low-set ears bilaterally. Their pectus carinatum remains prominent, as do as the surgical scars. (*F*) Profile views of twins. Both twins exhibit low-set, posteriorly rotated ears.

At 7 months, twin A underwent a liver transplant as well as inguinal and umbilical hernia repair. At 11 months, twin B underwent a liver transplant (complications included a right diaphragmatic hernia that was repaired at 14 months) and repair of the umbilical and inguinal hernias. At 21 months, twin A underwent a left-sided orchiopexy. At 2 years of age, both twins had atrial septum defect repair. They had multiple upper respiratory and ear infections even after bilateral myringotomy tubes were placed.

Both twins required early intervention services (physical therapy, occupational therapy, speech therapy, special instruction) because of mild developmental delays. By 3 years, all therapies were discontinued except for twin A's speech therapy. Over time, their facial features grew coarser. The probands continue to have significant pectus carinatum, cutis laxa, and hypermobility, with twin B's symptoms being more significant. However, no other remarkable clinical features were observed. Neither twin has developed signs of hearing loss.

Genomic Analyses

Postnatal findings of acute liver failure and jaundice led to suspicion of a mitochondrial hepatopathy, because hepatic involvement in childhood (primarily in the neonatal period) is a common feature in mitochondrial hepatopathies (Lee and Sokol 2007a,b). Mitochondrial DNA sequencing by next-generation sequencing (NGS) and mitochondrial DNA deletion

Table 1. *ATP6AP1* variants identified in the individuals in this study, with relevant population frequencies, total reads, variant allele fraction, inheritance, and classification

Genomic coordinates (hg19)	Reference allele	Alternative allele	Total reads	Variant allele fraction (VAF)	HGVS cDNA	HGVS protein (inheritance)	Zygosity	Variant type	gnomAD (v2.1.1) allele frequency	Variant classification
Chr X:153657459	CCTACT	CCT	120	100%	c.230_232delACT	p.Tyr77del (de novo)	Hemizygous	In-frame deletion	Absent	Likely pathogenic
Chr X:153657459	CCTACT	CCT	112	95%	c.230_232delACT	p.Tyr77del (de novo)	Hemizygous	In-frame deletion	Absent	Likely pathogenic

The Refseq transcript used for annotation is NM_001183.6.

and rearrangement by Southern blot did not show any pathogenic variants, deletions, or rearrangements.

Whole-exome sequencing (WES) was performed for both twins and included parental control samples. Overall WES achieved average coverage of 99.1% for probands and 97.9% for the father and mother for the coding region. Trio-based exome analysis identified a de novo hemizygous in-frame deletion (Chr X: 153657460delCTA, GRCh37/hg19) in the *ATP6AP1* gene present in both twins (Table 1). The variant (NM_001183.6: c.230_232delACT) is a 3-base pair deletion in exon 2 (out of 10 exons total) of the *ATP6AP1* gene, which causes an in-frame deletion of tyrosine at position 77 out of 471 amino acids total (NP_001174.2: p.Tyr77del). This variant was absent in the Genome Aggregation Database (gnomADV2.1.1). In silico analysis predicted the change to be deleterious to protein structure and/or function (PROVEAN score = −10.6). Sanger sequencing confirmed the presence of this de novo hemizygous variant in both affected twins. The variant was absent in both parents, although we cannot rule out the possibility of low-level gonadal mosaicism.

Literature and Database Review

To gain further insight into the spectrum of *ATP6AP1* variants associated with *ATP6AP1-CDG*-related disorders, we reviewed the literature and publicly available databases. In the ClinVar database, a total of 20 single-nucleotide variants (SNVs) in the *ATP6AP1* gene have been documented as pathogenic/likely pathogenic/variant of uncertain significance. Among them, 10 of the variants were reported to be associated with immunodeficiency 47 (OMIM #300972) *ATP6AP1-CDG*-related disorders. Of 20 reported single-nucleotide variants (SNVs), 19 are missense variants (95%) and one is a stop-gain variant (5%). The variants are distributed across all 10 exons and the predicted domains of the *ATP6AP1* gene, and there is no mutational hotspot observed in the gene (Fig. 2A,B). The overall intolerance of the *ATP6AP1* gene using all the seven missense variants reported in literature is plotted using missense tolerance ratio (MTR) viewer (Fig. 2C). We found that nine of the 10 (90%) disease-associated missense variants reside among the 50% most missense-intolerant sequence of the overall intolerant *ATP6AP1* gene. The MTR plot is based on standing variation data in the gnomAD database, version 2.0 (Silk et al. 2019).

Among 20 individuals (Jansen et al. 2016; Dimitrov et al. 2018; Witters et al. 2018; Gumm et al. 2020; Ondruskova et al. 2020; Tvina et al. 2020; Yang et al. 2021) summarized in Table 2 (18 reported in the literature and two from the current study), 17 showed hepatomegaly/liver failure/cirrhosis, 16 showed recurrent infection, 13 showed splenomegaly, 8 showed neurological symptoms, 6 showed cutis laxa, 5 were reported to have cardiac abnormalities or bilateral inguinal hernias, and 3 had a congenital diaphragmatic hernia. None of the individuals reported in the literature with *ATP6AP1-CDG* have been reported with

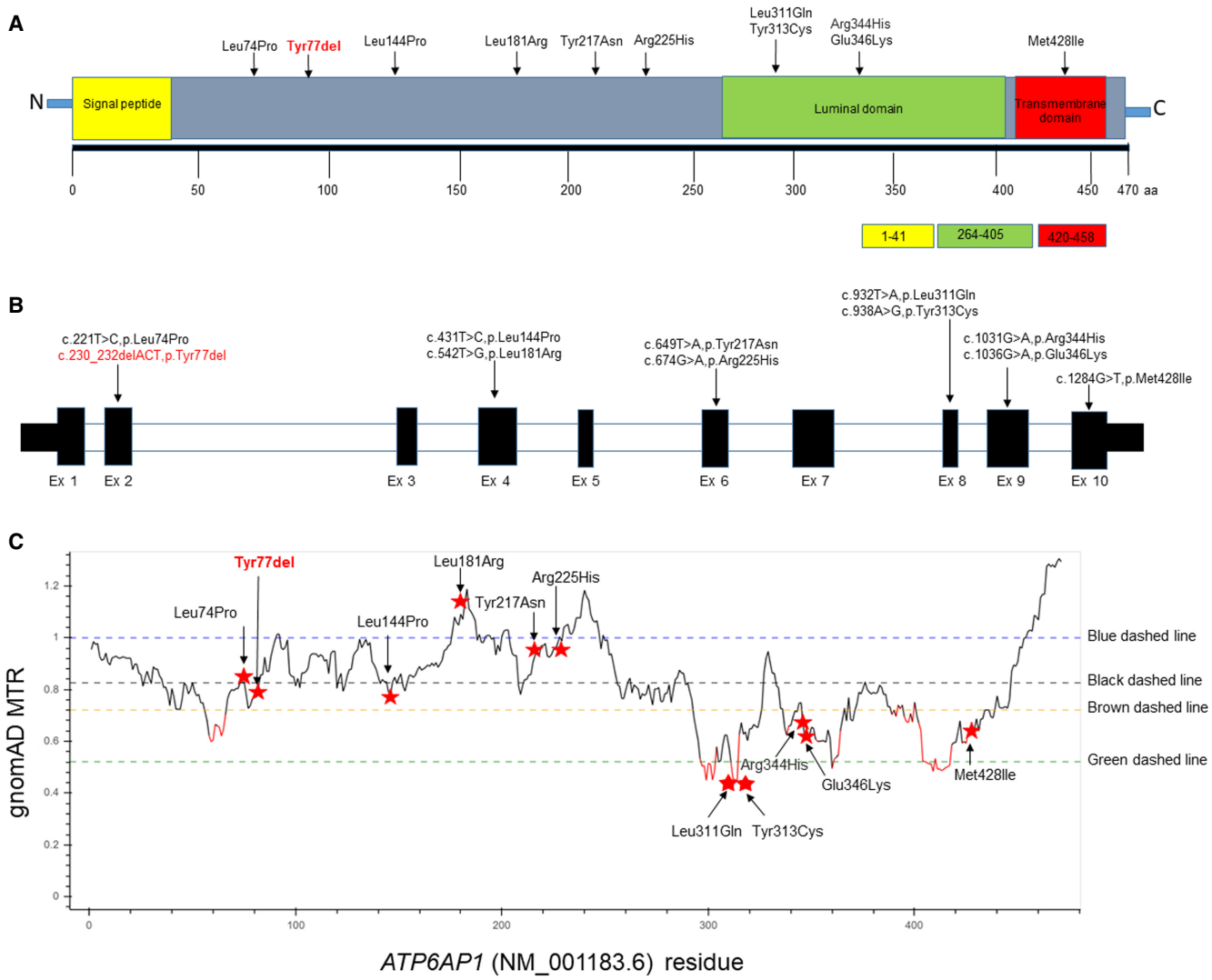

Figure 2. Schematic diagram representing distribution of variants across *ATP6AP1* (*A*) predicted functional domain and (*B*) exons (NM_001183.6). (Adapted from Jansen et al. 2016.) The in-frame deletion variant is represented in red. (*C*) The missense tolerance landscape (MTR) landscape of 10 case-ascertained *ATP6AP1* missense variants (denoted by red stars) calculated using the whole-exome sequencing (WES) component of gnomAD v2.0. The horizontal line shows gene-specific MTR percentile. An MTR = 1 (blue dashed) line represents neutrality (i.e., no positive/negative selection is occurring; the same proportion as expected is observed). The black dashed line represents MTR 50th percentile; the brown dashed line represents MTR 25th percentile; the green dashed line represents MTR 5th percentile.

ventriculomegaly, umbilical hernia, pectus carinatum, micropenis, or hypospadias, which we found in the probands in this study. Of note, to avoid bias by double counting, as the probands reported by Gumm et al. (2020) and Tvina et al. (2020) are the same set of siblings from a single family, they are counted only once in the phenotypic description.

Variant Classification

We assessed this in-frame deletion using a point-based approach following ACMG/AMP criteria (Version 1.0) updated recommendations for classifying de novo variants (PS2/

Table 2. Comparison of observed genetic and clinical findings of individuals from this study with patients reported with *ATP6AP1-CDG*-related congenital disorder

		Jansen et al. 2016										
		Family-1			Family-2	Family-3		Family-4		Family-5		Family-6
	HPO#	Individual 1	Individual 2	Individual 3	Individual 4	Individual 5	Individual 6	Individual 7	Individual 8	Individual 9	Individual 10	Individual 11
Age/ethnicity		20y/Caucasian	12y/Caucasian	34y/Caucasian	14 y/Caucasian	8 y/Druze	Died 4y/Druze	23 y/Caucasian	18 y/Caucasian	Died 12 mo /Tunisian	3 y/Tunisian	4 y/Irish
cDNAa/protein consequence		c.1284G > A; p.Met428Ile	c.1284G > A; p.Met428Ile	c.1284G > A; p.Met428Ile	c.431T > C; p.Leu144Pro	c.1036G > A; p.Glu346Lys	c.1036G > A; p.Glu346Lys	c.1036G > A; p.Glu346Lys	c.1036G > A; p.Glu346Lys	c.1036G > A; p.Glu346Lys	c.1036G > A; p.Glu346Lys	c.938 > 4G; p.Tyr313Cys
Variant type		Missense	Missense	Missense	Missense	Missense	Missense	Missense	Missense	Missense	Missense	Missense
Investigation method		WES/Sanger sequencing	WES/Sanger sequencing	WES/Sanger sequencing	WES	WES	Sanger sequencing	WES	Sanger sequencing	WES	Sanger sequencing	WES
Sex		Male	Male	Male	Male	Male	Male	Male	Male	Male	Male	Male
Inheritance		Maternal	Maternal	Maternal	Maternal	Maternal	Maternal	Maternal	Maternal	Maternal	Maternal	De novo
Fetal cystic hygroma	HP:0010878	ND	ND	ND	ND	ND	ND	ND	ND	ND	ND	ND
Fetal atrial septal defect/ dilated aorta/ cardiomegaly	HP:0001631; HP:0034058; HP:0001640	ND	ND	ND	ND	ND	ND	ND	ND	ND	ND	ND
Fetal ventriculomegaly	HP:0010952	ND	ND	ND	ND	ND	ND	ND	ND	ND	ND	ND
Cutis laxa	HP:0000973	ND	ND	ND	ND	ND	ND	ND	ND	ND	ND	ND
Hepatomegaly/liver failure/cirrhosis	HP:0001392	(+/-)	(-)	(-)	(-)	(+)	(+)	(+)	(+)	(+)	(+)	(+)
Splenomegaly	HP:0001744	(-)	(-)	(-)	(-)	(+)	(+)	(+)	(+)	(+)	(-)	(-)
Neurological symptoms	HP:0000707	(-)	(+/-)	(-)	(-)	(+)	(+)	(+)	(+)	(+)	(+)	(-)
Recurrent Infections	HP:0002719	(+)	(+)	(+)	(+)	(+)	(+)	(+)	(+)	(+)	(+)	(+)
Cardiac abnormalities	HP:0001627	ND	ND	ND	ND	ND	ND	ND	ND	ND	ND	ND
Bilateral inguinal hernias	HP:0000023	(+)	(+)	(+)	ND	ND	ND	ND	ND	ND	ND	ND
Umbilical hernia	HP:0001537	(-)	(-)	(-)	ND	ND	ND	ND	ND	ND	ND	ND
Diaphragmatic hernia	HP:0000776	ND	ND	ND	ND	ND	ND	ND	ND	ND	ND	ND
Pectus carinatum	HP:0000766	ND	ND	ND	ND	ND	ND	ND	ND	ND	ND	ND
Micropenis/hypospadias	HP:0000054; HP:0000047	ND	ND	ND	ND	ND	ND	ND	ND	ND	ND	ND

(*Continued on next page.*)

Table 2. (*Continued*)

		Imitrov et al. 2018	Witters et al. 2018	Tvina et al. 2020	Gumm et al. 2020	Ondruskova et al. 2020		Yang et al. 2021	This study		Consensus
	HPO#	Individual 12	Individual 13	Individual 14	Individual 15 (Case 1)	Individual 16	Individual 17	Individual 18	Twin A	Twin B	
Age/ethnicity		10 y/ND	5 mo/ND	38 wk (neonatal)/ND	5 mo/ND	Died 3 mo/ Caucasian Czech	Died 11 mo/ Caucasian Czech	8 mo/Chinese	4 y/Guyanese;Italian	4 y/Guyanese;Italian	
cDNAa/protein consequence		c.542T > G; p.Leu181Arg	c.649 T > A; p.Tyr217Asn	c.932T > A; p.Leu311Gln	c.932T > A; p.Leu311Gln	c.221T > C; p.Leu74Pro	c.221T > C; p.Leu74Pro	c.1036G > A; p.Glu346Lys	c.230_232delACT; p.Tyr77del	c.230_232delACT; p.Tyr77del	-
Variant type		Missense	Missense	Missense	Missense	Missense	Missense	Missense	In-frame deletion	In-frame deletion	-
Investigation method		WES	Sanger sequencing	WGS	WGS	WES/Sanger sequencing	WES/Sanger sequencing	WES	WES /Sanger sequencing	WES/Sanger sequencing	-
Sex		Male	Male	Male	Male	Male	Male	Male	Male	Male	20 of 20 (male)
Inheritance		Maternal	Maternal	Maternal	Maternal	Maternal	Maternal	De novo	De novo	De novo	4 of 20 (de novo)
Fetal cystic hygroma	HP:0010878	ND	ND	Thickened nuchal translucency (–)	ND	ND	ND	ND	(+)	(+)	3 of 3
Fetal atrial septal defect/ dilated aorta/ cardiomegaly	HP:0001631; HP:0034058; HP:0001640	ND	ND	Dilated aorta, atrial septal defect (+)	ND	ND	ND	ND	(+)	(+)	3 of 3
Fetal ventriculomegaly	HP:0010952	ND	ND	ND	ND	ND	ND	ND	(+)	(+)	2 of 2
Cutis laxa	HP:0000973	(+)	(+)	(–)	(-)	(+)	(+)	(-)	(+)	(+)	7 of 9
Hepatomegaly/liver failure/ cirrhosis	HP:0001392	(+)	(+)	(+)	(+)	(+)	(+)	(+)	Liver failure (+)	Liver failure (+)	17 of 20
Splenomegaly	HP:0001744	(+)	(+)	(-)	(+)	(+)	(+)	(+)	(+)	(+)	13 of 20
Neurological symptoms	HP:0000707	(-)	(-)	(-)	(-)	(-)	(-)	(+)	(-)	(-)	8 of 20
Recurrent Infections	HP:0002719	(+)	(+)	(-)	(-)	(-)	(-)	(+)	(+)	(+)	16 of 20
Cardiac abnormalities	HP:0001627	(+)	(+)	(+)	(-)	ND	ND	(-)	(+)	(+)	5 of 7
Bilateral inguinal hernias	HP:0000023	ND	(-)	ND	ND	ND	ND	(-)	(+)	(+)	5 of 7
Umbilical hernia	HP:0001537	ND	(-)	ND	ND	ND	ND	(-)	(+)	(+)	2 of 7
Diaphragmatic hernia	HP:0000776	ND	(+)	ND	ND	ND	ND	(-)	(+)	(+)	3 of 4
Pectus carinatum	HP:0000766	ND	ND	ND	ND	ND	ND	ND	(+)	(+)	2 of 2
Micropenis/hypospadias	HP:0000054; HP:0000047	ND	ND	ND	ND	ND	ND	ND	(+)	(+)	2 of 2

Unique features observed in this current study are highlighted in blue.
(WES) Whole-exome sequencing, (WGS) whole-genome sequencing, (ND) no data, (+) present, (–) absent, (+/–) indicated as such in the table outlining the clinical features of that individual in the original publication. Rows in gray highlight the unique features observer in the patients reported in this study.

PM6) published March 2018 (SVI 2018). Considering the overlapping features and consistent hepatic findings in all reported individuals, we used the strength level of strong, with a total of two points. Moreover as p.Tyr77del is a single-amino acid in-frame deletion, we downgraded the moderate level PM4 criteria to a supporting level of evidence following the ACGS framework (ACGS 2019). As this variant is absent in the population database, we implied the recommended supporting level evidence of PM2. Using these recommendations as a framework from various working groups, the c.230_232delACT;p.Tyr77del was classified as likely pathogenic.

DISCUSSION

There are 18 individuals reported in the literature with *ATP6AP1-CDG*-related disorder with missense variants in the *ATP6AP1* gene (Jansen et al. 2016; Dimitrov et al. 2018; Witters et al. 2018; Ondruskova et al. 2020; Song et al. 2020; Tvina et al. 2020). The most striking clinical features shared among all reported cases is liver disease that varies from increased transaminase to steatosis, cirrhosis, or/and cholestasis. This is similar to other CDGs reported in the literature (Starosta et al. 2021). Immunodeficiency is also commonly reported. Although the initial case series in 2016 reported neurological symptoms as a component of the phenotype, the neurological features were only present in individuals with one specific variant (p.Glu346Lys), and no cases reported since, including this one, have included neurological features. However, there have been multiple cases, including our own, that have noted cutis laxa as a significant feature of *ATP6AP1-CDG*-related disorder. Both twins in this case study presented with significant connective tissue features, including velvety soft skin with laxity, especially in the epigastric and groin/flank regions, pectus carinatum, inguinal and umbilical hernias, and a dilated ascending aorta. Furthermore, the prenatal features seen in these twins are consistent with the previously reported prenatal phenotype of dilated ascending aorta (Tvina et al. 2020); however, our patients also presented with cystic hygroma, atrial septal defect, and ventriculomegaly prenatally. Thus, our case further affirms that although the connective tissue and prenatal findings are likely more common than previously assessed, neurological features do not appear to be central in *ATP6AP1-CDG*-related disorder.

Similar to a patient recently reported (Gumm et al. 2020; Tvina et al. 2020), the probands presented in this study did not demonstrate any defects in glycosylation, which was performed after liver transplantation. Indeed, Gumm et al. reported that although the same variant was present in two siblings, it showed an abnormal glycosylation in one of the probands, whereas it was normal in the other proband. The observation of normal glycosylation patterns in two independent studies may indicate that although a clinical indication could be remarkable, not all patients with a significant variant in the *ATP6AP1* gene (which functions primarily in luminal acidification of the secretory vesicle) will necessarily exhibit abnormal glycosylation patterns. This may also indicate that in the case of a strong clinical suspicion for *ATP6AP1-CDG*-related disorder, sequencing should be included as part of the evaluation, even in patients with a normal glycosylation profile. Indeed, variability in glycosylation patterns in patients with *ATP6AP1-CDG* have also been reported by Jansen et al. and diagnosis of CDG with a normal glycosylation pattern has been reported in other known types of CDG in the literature (Zuhlsdorf et al. 2015). Although cutis laxa with minimum neurological findings is not enough to differentiate *ATP6AP1-GDG* from other V-ATPases, these findings, along with hepatic dysfunction, should raise enough suspicion to think of the particular condition regardless of transferrin glycosylation studies.

Excluding this case, all previously reported SNVs associated with *ATP6AP1-CDG*-related disorders were missense variants. Although a functional study on patient fibroblasts harboring a missense (c.542T > G, p.Leu181Arg) variant has excluded apoptosis as a cause, there

was significant elongation of doubling time and reduced proliferation of fibroblasts observed (Dimitrov et al. 2018). Our patients have a 3-bp in-frame deletion that eliminates a single tyrosine residue and leads to a clinical phenotype consistent with *ATP6AP1-CDG*-related disorder.

When WES was done initially in 2016, the de novo in-frame deletion (c.230_232delACT; p.Tyr77del) identified in our patients was classified as variant of uncertain significance. This classification was based on the data and evidence available at that point of time. However, clinical reevaluation of these two siblings in 2020, together with updated recommendations on variant interpretation (SVI 2018; ACGS 2019) and additional evidence of case-level data from recent literature, showed an overlapping phenotype associated with *ATP6AP1-CDG*, which resulted in reclassification of this variant to likely pathogenic. Our results support the importance of long-term clinical follow-up of individuals with rare diseases and reinterpretation of rare variants based on emerging evidence and updated guidelines/recommendations, which has the potential to alter overall management. Although it is a limitation in this study, in the future, determination of the consequences of the tyrosine deletion on overall structure and folding of the *ATP6AP1* might reveal additional information on the potential function of this subunit on the V-ATPase complex.

Conclusion

In conclusion, we present two additional individuals with *ATP6AP1-CDG*-related congenital disorder of glycosylation due to a novel de novo in-frame deletion. Our case extends the knowledge of clinical manifestations in the prenatal and postnatal stages, which increases the understanding and knowledge about this rare disorder. It further affirms that neurological features do not seem to be central to this condition, and that cutis laxa as well as other connective tissue features are more prevalent. Moreover, it highlights the impact of variant reinterpretation with implementation of updated guidelines/recommendations and its clinical implication on long-term patient care and genetic counseling.

METHODS

Whole-Exome Sequencing (WES) and Analysis

WES was performed after written informed consent was obtained, at the Laboratory of Personalized Genomic Medicine at Columbia University Irving Medical Center on DNA obtained from peripheral blood of both twins as well as their parents. Paired-end sequencing was performed on the Illumina HiSeq 2500 platform using Agilent SureSelectXT (Human All Exon v.5 + UTRs) capture kit following manufacturers' protocol. NextGENe (version 2.3; SoftGenetics, LLC) software was used to align (hg19) and annotate the sequence data. Variants were filtered and annotated using a New York State–approved in-house-developed pipeline. Variants were reviewed as part of the workflow for constitutional clinical exome sequencing in the Laboratory of Personalized Genomic Medicine at Columbia University Medical Center as previously described (Kurtz et al. 2021).

ADDITIONAL INFORMATION

Data Deposition and Access

The variants were submitted to ClinVar (https://www.ncbi.nlm.nih.gov/clinvar/) and can be found under accession number VCV001686802.1.

Ethics Statement

Clinical genetic testing was performed with informed consent. Parental consent was obtained for publication of clinical features and photographs of the twins, probands (P) 1 and 2. Clinical testing does not require IRB approval.

Acknowledgments

The authors thank the probands and their family for participating in this study.

Author Contributions

S.Ba. analyzed genomic WES data, investigated, wrote the original draft, and reviewed and edited the manuscript. S.Be. performed genetic counseling, data extraction from the medical records, and reviewed and edited the manuscript. E.M.P. performed the data extraction from the medical records, examined and followed-up with the probands, supervised the project, and wrote, reviewed and edited the manuscript. V.J. performed formal analysis of the genomic WES data, supervised the project, and reviewed and edited the manuscript. All authors revised, contributed intellectually, and approved the final version of the manuscript.

Competing Interest Statement

The authors have declared no competing interest.

Received January 13, 2022; accepted in revised form April 8, 2022.

Funding

This research did not receive any specific grant support.

REFERENCES

ACGS Best Practice Guidelines for Variant Classification. 2019. https://www.acgs.uk.com/quality/best-practice-guidelines/

Cannata Serio M, Graham LA, Ashikov A, Larsen LE, Raymond K, Timal S, Le Meur G, Ryan M, Czarnowska E, Jansen JC, et al. 2020. Mutations in the V-ATPase assembly factor VMA21 cause a congenital disorder of glycosylation with autophagic liver disease. *Hepatology* **72:** 1968–1986. doi:10.1002/hep.31218

Casey JR, Grinstein S, Orlowski J. 2010. Sensors and regulators of intracellular pH. *Nat Rev Mol Cell Biol* **11:** 50–61. doi:10.1038/nrm2820

Chang IJ, He M, Lam CT. 2018. Congenital disorders of glycosylation. *Ann Transl Med* **6:** 477. doi:10.21037/atm.2018.10.45

Dimitrov B, Himmelreich N, Hipgrave Ederveen AL, Luchtenborg C, Okun JG, Breuer M, Hutter AM, Carl M, Guglielmi L, Hellwig A, et al. 2018. Cutis laxa, exocrine pancreatic insufficiency and altered cellular metabolomics as additional symptoms in a new patient with *ATP6AP1-CDG*. *Mol Genet Metab* **123:** 364–374. doi:10.1016/j.ymgme.2018.01.008

Guillard M, Dimopoulou A, Fischer B, Morava E, Lefeber DJ, Kornak U, Wevers RA. 2009. Vacuolar H+-ATPase meets glycosylation in patients with cutis laxa. *Biochim Biophys Acta* **1792:** 903–914. doi:10.1016/j.bbadis.2008.12.009

Gumm AJ, Basel DG, Thakrar P, Suchi M, Telega G. 2020. Liver failure and X-linked immunodeficiency type 47. *Pediatr Transplant* **24:** e13808. doi:10.1111/petr.13808

Jansen EJ, Timal S, Ryan M, Ashikov A, van Scherpenzeel M, Graham LA, Mandel H, Hoischen A, Iancu TC, Raymond K, et al. 2016. *ATP6AP1* deficiency causes an immunodeficiency with hepatopathy, cognitive impairment and abnormal protein glycosylation. *Nat Commun* **7:** 11600. doi:10.1038/ncomms11600

Kornak U, Reynders E, Dimopoulou A, van Reeuwijk J, Fischer B, Rajab A, Budde B, Nurnberg P, Foulquier F, Group AD-tS, et al. 2008. Impaired glycosylation and cutis laxa caused by mutations in the vesicular H+-ATPase subunit ATP6V0A2. *Nat Genet* **40:** 32–34. doi:10.1038/ng.2007.45

Kurtz J, Fernandes JA Jr, Mansukhani M, Copeland WC, Naini AB. 2021. Whole-exome sequencing identifies a novel POLG frameshift variant in an adult patient presenting with progressive external ophthalmoplegia and mitochondrial DNA depletion. *Case Rep Genet* **2021:** 9969071. doi:10.1155/2021/9969071

Lee WS, Sokol RJ. 2007a. Liver disease in mitochondrial disorders. *Semin Liver Dis* **27:** 259–273. doi:10.1055/s-2007-985071

Lee WS, Sokol RJ. 2007b. Mitochondrial hepatopathies: advances in genetics and pathogenesis. *Hepatology* **45:** 1555–1565. doi:10.1002/hep.21710

Ng BG, Freeze HH. 2018. Perspectives on glycosylation and its congenital disorders. *Trends Genet* **34:** 466–476. doi:10.1016/j.tig.2018.03.002

Nishi T, Forgac M. 2002. The vacuolar (H+)-ATPases—nature's most versatile proton pumps. *Nat Rev Mol Cell Biol* **3:** 94–103. doi:10.1038/nrm729

Ondruskova N, Honzik T, Vondrackova A, Stranecky V, Tesarova M, Zeman J, Hansikova H. 2020. Severe phenotype of *ATP6AP1-CDG* in two siblings with a novel mutation leading to a differential tissue-specific ATP6AP1 protein pattern, cellular oxidative stress and hepatic copper accumulation. *J Inherit Metab Dis* **43:** 694–700. doi:10.1002/jimd.12237

Pamarthy S, Kulshrestha A, Katara GK, Beaman KD. 2018. The curious case of vacuolar ATPase: regulation of signaling pathways. *Mol Cancer* **17:** 41. doi:10.1186/s12943-018-0811-3

Rujano MA, Cannata Serio M, Panasyuk G, Peanne R, Reunert J, Rymen D, Hauser V, Park JH, Freisinger P, Souche E, et al. 2017. Mutations in the X-linked *ATP6AP2* cause a glycosylation disorder with autophagic defects. *J Exp Med* **214:** 3707–3729. doi:10.1084/jem.20170453

Silk M, Petrovski S, Ascher DB. 2019. MTR-Viewer: identifying regions within genes under purifying selection. *Nucl Acids Res* **47:** W121–W126. doi:10.1093/nar/gkz457

Song Q, Meng B, Xu H, Mao Z. 2020. The emerging roles of vacuolar-type ATPase-dependent lysosomal acidification in neurodegenerative diseases. *Transl Neurodegener* **9:** 17. doi:10.1186/s40035-020-00196-0

Starosta RT, Boyer S, Tahata S, Raymond K, Lee HE, Wolfe LA, Lam C, Edmondson AC, Schwartz IVD, Morava E. 2021. Liver manifestations in a cohort of 39 patients with congenital disorders of glycosylation: pin-pointing the characteristics of liver injury and proposing recommendations for follow-up. *Orphanet J Rare Dis* **16:** 20. doi:10.1186/s13023-020-01630-2

SVI Recommendation for De Novo Criteria (PS2 & PM6)—Version 1.0. https://clinicalgenome.org/working-groups/sequence-variant-interpretation/

Tvina A, Thomsen A, Palatnik A. 2020. Prenatal and postnatal phenotype of a pathologic variant in the *ATP6AP1* gene. *Eur J Med Genet* **63:** 103881. doi:10.1016/j.ejmg.2020.103881

Van Damme T, Gardeitchik T, Mohamed M, Guerrero-Castillo S, Freisinger P, Guillemyn B, Kariminejad A, Dalloyaux D, van Kraaij S, Lefeber DJ, et al. 2017. Mutations in *ATP6V1E1* or *ATP6V1A* cause autosomal-recessive cutis laxa. *Am J Hum Genet* **100:** 216–227. doi:10.1016/j.ajhg.2016.12.010

Wilson MP, Matthijs G. 2021. The evolving genetic landscape of congenital disorders of glycosylation. *Biochim Biophys Acta Gen Subj* **1865:** 129976. doi:10.1016/j.bbagen.2021.129976

Witters P, Breckpot J, Foulquier F, Preston G, Jaeken J, Morava E. 2018. Expanding the phenotype of metabolic cutis laxa with an additional disorder of N-linked protein glycosylation. *Eur J Hum Genet* **26:** 618–621. doi:10.1038/s41431-017-0044-8

Yang X, Lv Z-L, Tang Q, Chen X-Q, Huang L, Yang MX, Lan L-C, Shan Q-W. 2021. Congenital disorder of glycosylation caused by mutation of *ATP6AP1* gene (c.1036G>A) in a Chinese infant: case report. *World J Clin Diseases* **9:** 7876–7885. doi:10.12988/wjcc.v9.i26.7876

Zuhlsdorf A, Park JH, Wada Y, Rust S, Reunert J, DuChesne I, Gruneberg M, Marquardt T. 2015. Transferrin variants: pitfalls in the diagnostics of congenital disorders of glycosylation. *Clin Biochem* **48:** 11–13. doi:10.1016/j.clinbiochem.2014.09.022